generations. The transgene was routinely identified using genomic PCR with tail DNAs (Fig. 1B). In Southern blotting, the number of transgenes was roughly 10 copies per genome (Fig. 1C). In the sciatic nerve lysates, expression levels of ErbB3, but not ErbB2, were approximately 70% lower in transgenic mice compared to their littermate controls (Fig. 1D and E). In contrast, no effect of ErbB3 knockdown was seen in the whole brain (Fig. 1F), indicating that the knockdown occurs in the peripheral nervous system only.

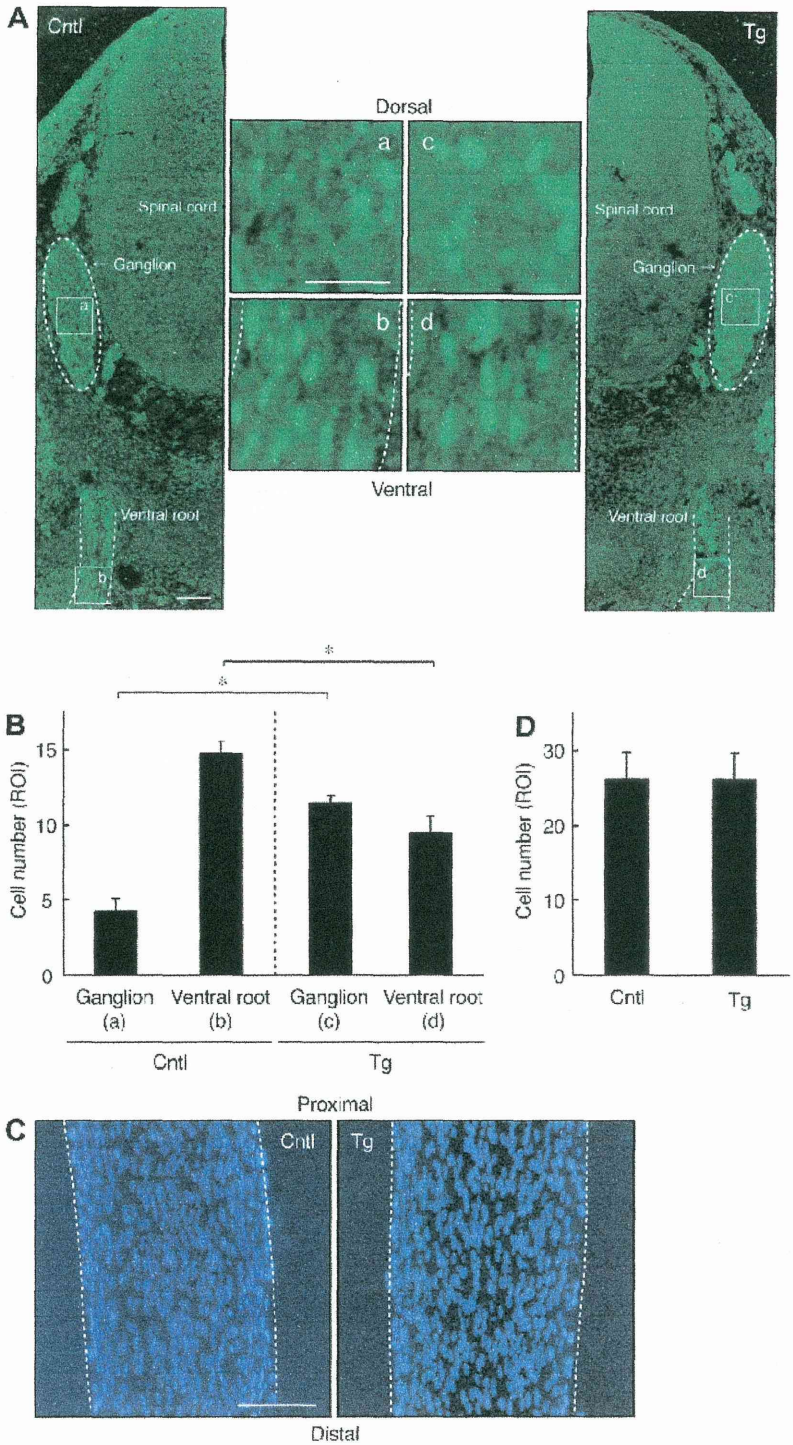

Fig. 2. ShErbB3 transgenic mice exhibit delayed migration from ganglia to ventral roots. (A) Dorsoventral sections of control mice (Cntl) and transgenic mice (Tg) at embryonic day 12.5 were stained with an anti-Sox10 antibody. Central panels a–d are enlarged images of the positions indicated by white squares a–d in the left and right panels. Peripheral nerve outlines are indicated by white dotted lines. (B and D) The number of Sox10- or DAPI-positive cells in each 200 μm-square field was counted and is shown in the graph (*$p < 0.01$; $n = 4$). (C) Vertical sections of sciatic nerves at postnatal day 7 were stained with DAPI (blue). Scale bars indicate 100 μm.

To investigate whether ErbB3 regulates Schwann cell precursor migration in mouse embryos, we produced a tissue slice that was cut along a dorsoventral axis. A dorsoventral root from a ganglion is one of the major migration roots in Schwann cell precursors [1,2]. At embryonic day 12.5, Schwann cell lineage cell's marker Sox10-positive cells in ErbB3 shRNA transgenic mice exhibited delayed migration along a route from the ganglion to the ventral root (Fig. 2A). The number of Sox10-positive cells in ErbB3 shRNA transgenic mouse ganglia was greater than that in the controls (panel c compared to panel a in Fig. 2A; 3rd lane compared to 1st lane in Fig. 2B). In contrast, the opposite phenomenon was observed in the ventral roots (panel d compared to panel b in Fig. 2A; 4th lane compared to 2nd lane in Fig. 2B). After birth, the number of DAPI-positive cells in the sciatic nerves was comparable in transgenic mice and the controls (Fig. 2C and D). Both Schwann cells and neuronal axons are contained in the sciatic nerves where DAPI-positive nucleus are mainly present in Schwann cells. Thus, ErbB3 is required for Schwann cell precursor migration *in vivo*; however, it is unlikely that ErbB3 knockdown affects cell proliferation in transgenic mice (Fig. S1). Next, we isolated Schwann cell precursors from mouse embryos and asked whether Erb3 is involved in their migration *in vitro*. Schwann cell precursors were reaggregated and allowed to migrate out onto dishes. The reaggregates from ErbB3 shRNA transgenic mice exhibited decreased migration, compared to the controls (Fig. 3A and B), consistent with our finding that ErbB3 is required for Schwann cell precursor migration *in vivo*.

To confirm that ErbB3 contributes to Schwann cell myelination in this transgenic mouse, we performed ultrastructural analysis of sciatic nerves. Myelination in the PNS begins within couples of days after birth and remains active until around 2 months of age [1,2]. Electron microscopic analysis illustrated that sciatic nerves from 3.5-day-old shErbB3 transgenic mice exhibited decreased myelin thickness compared to those from the controls (Fig. 4A). The decreased myelin thickness in transgenic mice is clearly evident from quantification of the g-ratio, that is the numerical ratio between the axon diameter and the outer myelinated fiber diameter (Fig. 4B). Thinner myelin layers yield larger g-ratio values.

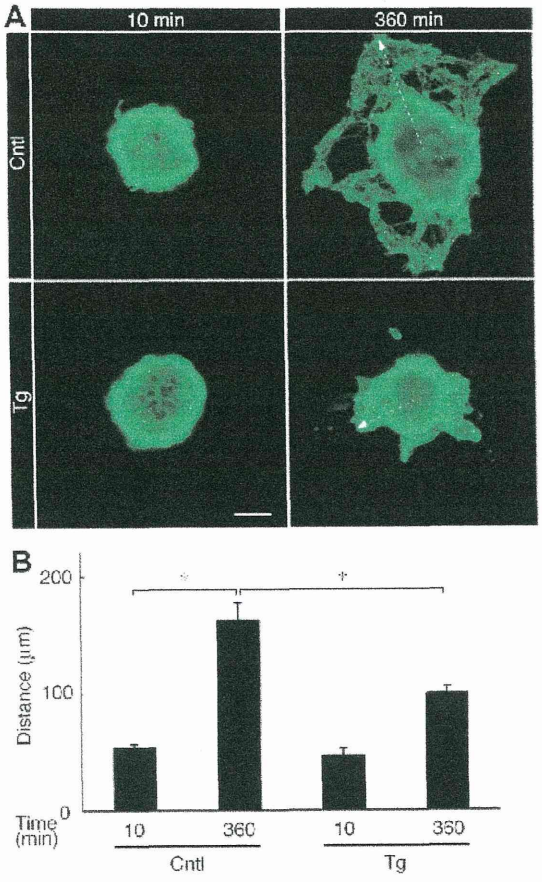

Fig. 3. Knockdown of ErbB3 inhibits migration from Schwann cell precursor reaggregates. (A and B) Schwann cell precursors from control mice (Cntl) and transgenic mice (Tg) were reaggregated and allowed to migrate from reaggregates for 6 h. Cells were stained with an anti-p75 neurotrophin receptor antibody (green). The distance from the center of the reaggregate was considered the migrating distance and was measured. The representative migrating direction and distance are shown in a white dotted arrow. The distance is shown in the graph (*$p < 0.01$; $n = 3$). Scale bar indicates 50 μm. (For interpretation of the references to color in this figure legend, the reader is referred to the web version of this article.)

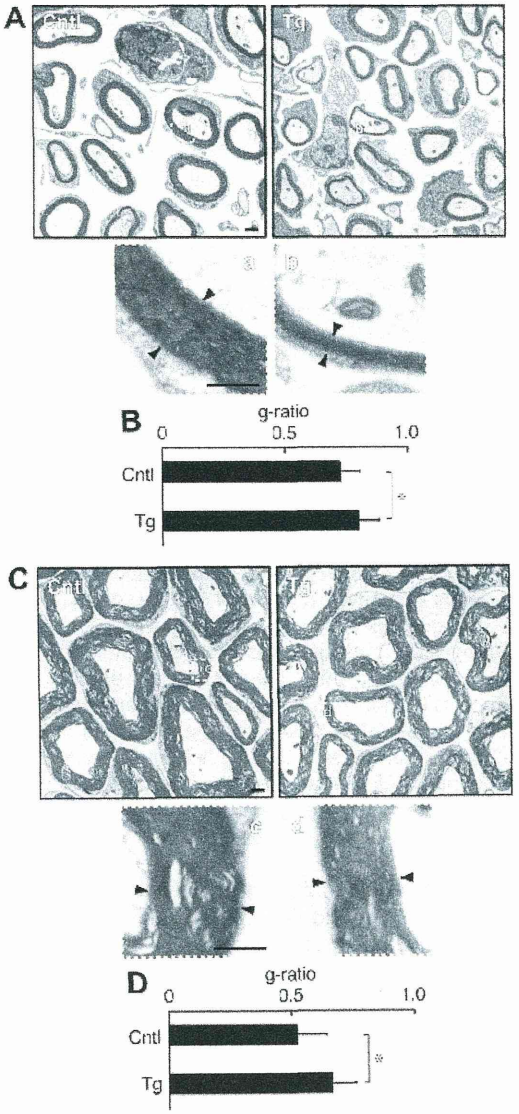

Fig. 4. ShErbB3 transgenic mice exhibit delayed myelination. Electron micrographs of sciatic nerve cross sections in control mice (Cntl) and transgenic mice (Tg) at postnatal day 3.5 (A) and 56 (C) are shown. (A and C) Lower panels a–d are enlarged images of the positions indicated by white dotted squares a–d in the upper panels. Distance between arrowheads indicates representative myelin sheath thickness. Scale bars indicate 1 μm. (B and D) The ratios of axon diameters to outer myelinated axon diameters are shown (*$p < 0.01$; n = more than 50).

Similar results were observed in 56-day-old transgenic mice (Fig. 4C and D). We finally established Schwann cell-neuronal cultures from transgenic mice and the controls to confirm that ErbB3 knockdown reduces myelination *in vitro*. After around 2-week-culture following addition of ascorbic acid, we stained myelin segments with an antibody against MBP, which is the myelin marker protein. Knockdown of ErbB3 inhibited myelination by more than 80% (Fig. S2), consistent with our finding that ErbB3 is required for Schwann cell myelination *in vivo*.

4. Discussion

Schwann cell precursors proliferate, migrate to their final destinations, and differentiate for myelination of the peripheral neuronal axons. In zebrafish, a transparent experimental model animal, genetic studies have illustrated that the ligand-binding ErbB3 receptor is required for Schwann cell precursor proliferation and migration along peripheral axons, as well as for myelination [5,15]. In mice, complete knockout of ErbB3 results in embryonic lethality with a complete loss of Schwann cell precursors; its effects are similar to those of various peripheral neuropathy symptoms involving Schwann cell precursor loss [16,17], indicating that ErbB3 is essential for cell growth and/or survival of the precursors. Although ErbB3 is known to play several roles in Schwann cell lineage cell development, it remains unclear whether ErbB3 is actually required for migration in mammals. Here, we show that ErbB3 knockdown does not lead to lethality; rather, it delays Schwann cell precursor migration. This finding is consistent with the results of our *in vitro* migration assay. Therefore, our results indicate that the role of ErbB3 in migration is conserved in mammals.

Schwann cell-specific ErbB3 shRNA transgenic mice are not lethal, probably since ErbB3 expression is not completely blocked in these transgenic mice. A similar phenotype of mildly reduced myelin thickness is also seen in the Schwann cell developmental stage following migration. On the other hand, like mice with complete ErbB3 knockout, mice with knockout of the cognate ligand, NRG1 type III, display embryonic lethality with a loss of Schwann cell precursors [18]. Since peripheral neurons express NRG1 type III, peripheral neuron-specific NRG1 type III shRNA transgenic mice may allow us to analyze the role of NRG1 type III, as the ErbB3 ligand, in Schwann cell precursor migration. Transgenic mice transcribing shRNA using a tissue-specific promoter are called shRNAmir transgenic mice [7,8]. Although tissue-specific RNA interference does not completely suppress expression of the target molecule, it is useful for analyzing the role of an intended gene *in vivo* [7,8]. In particular, it may be helpful to produce shRNAmir transgenic mice before evaluating the intended gene using conditional knockout mice, since the length of time required to produce transgenic mice is much shorter than that required to produce knockout mice.

In addition to neuregulin-1, growth factors such as neurotrophin-3 [2,6,19] and insulin-like growth factor 1 [2,6,20] are known to be provided by peripheral neurons. They bind to the respective cognate receptors on Schwann cells and promote Schwann cell precursor migration, although these roles have only been demonstrated in *in vitro* experimental systems. Transgenic mice transcribing shRNA using each peripheral neuron- or Schwann cell-specific promoter may be useful in determining whether the relationship between previously unknown growth factors and receptors actually contributes to migration *in vivo*.

It is clear that ErbB3 is required for Schwann cell precursor migration, but the downstream signal transducers are not thoroughly understood. A possible signal transducer seems likely to be non-receptor type protein tyrosine phosphatase 11 (PTPN11, also called Shp2). PTPN11 is a binding partner of the ErbB family, and PTPN11 mutant mice display not only reduced myelin thickness but also impaired Schwann cell precursor migration [21]. PTPN11 dephosphorylates the negative phosphorylated tyrosine residues of non-receptor type Src family tyrosine kinases including Fyn, resulting in the activation of Src family kinases *in vitro* and *in vivo* [22]. Fyn is an important regulator not only in the development of oligodendrocytes, myelin-forming glial cells in the central nervous system, but also in Schwann cell development [9,23]. It is conceivable that PTPN11 couples with ErbB2/3 to activate Fyn, leading to the promotion of Schwann cell precursor migration. In addition, it is noteworthy that, in PTPN11 mutant precursors, the activity of extracellular signal-regulated kinase (ERK), the major intracellular signal convergent molecule, is greatly inhibited [21]. ERK plays a key role in migration in many cell types by phosphorylating many actin and tubulin cytoskeletal proteins and their associated molecules [24]. Thus, ERK may act downstream of ErbB2/3 and PTPN11, contributing to Schwann cell precursor migration.

In this study, we show that in mice, the ligand-binding ErbB3 is required for Schwann cell precursor migration, and thus that ErbB3 plays a conservative role in PNS glial cell migration. Further studies will clarify the detailed molecular mechanisms by which ErbB2/3 regulates migration. It would be interesting to investigate whether the ErbB2/3 receptor and the underlying signaling pathway may be also involved in migration following injury, since cell migration is often observed following injury as well as during development. Such studies on the mechanisms controlling migration may help us to elucidate a paradigm for remyelination processes and nerve regeneration.

Acknowledgments

We thank Drs. Y. Matsubara and H. Saito (National Research Institute for Child Health and Development) for helpful discussions and encouragement. We also thank Drs. W. Fumanski and C. Rowthorn (Eibunkousei.net, Inc.) for reading this manuscript. This work was supported by Grants-in-Aid for Young Scientists, Scientific Research B, and Scientific Research on Innovative Areas (Glial assembly: a new regulatory machinery of brain function and disorders) from the Japanese Ministry of Education, Culture, Sports, Science, and Technology (MEXT). This work was also supported by Grants-in-Aid for Scientific Research from the Japanese Ministry of Health, Labor, and Welfare (MHLW) and partially by the Takeda Science Foundation.

Appendix A. Supplementary data

Supplementary data associated with this article can be found, in the online version, at http://dx.doi.org/10.1016/j.bbrc.2014.08.156.

References

[1] R.P. Bunge, Expanding roles for the Schwann cell: ensheathment, myelination, trophism and regeneration, Curr. Opin. Neurobiol. 3 (1993) 805–809.
[2] R. Mirsky, K.R. Jessen, Schwann cell development, differentiation and myelination, Curr. Opin. Neurobiol. 6 (1996) 89–96.
[3] K.A. Nave, J.L. Salzer, Axonal regulation of myelination by neuregulin 1, Curr. Opin. Neurobiol. 16 (2006) 492–500.
[4] C. Taveggia, M.L. Feltri, L. Wrabetz, Signals to promote myelin formation and repair, Nat. Rev. Neurol. 6 (2010) 276–287.
[5] A.R. Raphael, W.S. Talbot, New insights into signaling during myelination in zebrafish, Curr. Top. Dev. Biol. 97 (2011) 1–19.
[6] Y. Miyamoto, J. Yamauchi, Recent insights into molecular mechanisms that control growth factor receptor-mediated Schwann cell morphological changes during development, in: K. Sango, J. Yamauchi (Eds.), Schwann Cell Development and Pathology, Springer, 2014, pp. 5–27 (Chapter 2).
[7] S. Gu, L. Jin, Y. Zhang, Y. Huang, F. Zhang, P.N. Valdmanis, M.A. Kay, The loop position of shRNAs and pre-miRNAs is critical for the accuracy of Dicer processing in vivo, Cell 151 (2012) 900–911.

[8] C. Fellmann, T. Hoffmann, V. Sridhar, B. Hopfgartner, M. Muhar, M. Roth, D.Y. Lai, I.A. Barbosa, J.S. Kwon, Y. Guan, N. Sinha, J. Zuber, An optimized microRNA backbone for effective single-copy RNAi, Cell Rep. 5 (2013) 1704–1713.
[9] J. Yamauchi, Y. Miyamoto, T. Torii, S. Takashima, K. Kondo, K. Kawahara, N. Nemoto, J.R. Chan, G. Tsujimoto, A. Tanoue, Phosphorylation of cytohesin-1 by Fyn is required for initiation of myelination and the extent of myelination during development, Sci. Signal. 5 (2012) ra69.
[10] Y. Miyamoto, T. Torii, N. Yamamori, T. Ogata, A. Tanoue, J. Yamauchi, Akt and PP2A reciprocally regulate the guanine nucleotide exchange factor Dock6 to control axon growth of sensory neurons, Sci. Signal. 6 (2013) ra15.
[11] N. Ratner, J.P. Williams, J.J. Kordich, K.A. Kim, Schwann cell preparation from single mouse embryos: analyses of neurofibromin function in Schwann cells, Methods Enzymol. 407 (2006) 22–33.
[12] Y. Miyamoto, T. Torii, K. Nakamura, S. Takashima, A. Sanbe, A. Tanoue, J. Yamauchi, Signaling through Arf6 guanine-nucleotide exchange factor cytohesin-1 regulates migration in Schwann cells, Cell. Signal. 25 (2013) 1379–1387.
[13] M.L. Feltri, M. D'Antonio, S. Previtali, M. Fasolini, A. Messing, L. Wrabetz, P0-Cre transgenic mice for inactivation of adhesion molecules in Schwann cells, Ann. N. Y. Acad. Sci. 883 (1999) 116–123.
[14] Y. Yamauchi, K. Abe, A. Mantani, Y. Hitoshi, M. Suzuki, F. Osuzu, S. Kuratani, K. Yamamura, A novel transgenic technique that allows specific marking of the neural crest cell lineage in mice, Dev. Biol. 212 (1999) 191–203.
[15] D.A. Lyons, H.M. Pogoda, M.G. Voas, I.G. Woods, B. Diamond, R. Nix, N. Arana, J. Jacobs, W.S. Talbot, Erbb3 and Erbb2 are essential for Schwann cell migration and myelination in zebrafish, Curr. Biol. 15 (2005) 513–524.
[16] D. Riethmacher, E. Sonnenberg-Riethmacher, V. Brinkmann, T. Yamaai, G.R. Lewin, C. Birchmeier, Severe neuropathies in mice with targeted mutations in the ErbB3 receptor, Nature 389 (1997) 725–730.
[17] S.L. Erickson, K.S. O'Shea, N. Ghaboosi, L. Loverro, G. Frantz, M. Bauer, L.H. Lu, M.W. Moore, ErbB3 is required for normal cerebellar and cardiac development: a comparison with ErbB2- and heregulin-deficient mice, Development 124 (1997) 4999–5011.
[18] D. Wolpowitz, T.B. Mason, P. Dietrich, M. Mendelsohn, D.A. Talmage, L.W. Role, Cysteine-rich domain isoforms of the neuregulin-1 gene are required for maintenance of peripheral synapses, Neuron 25 (2000) 79–91.
[19] J. Yamauchi, J.R. Chan, E.M. Shooter, Neurotrophin 3 activation of TrkC induces Schwann cell migration through the c-Jun N-terminal kinase pathway, Proc. Natl. Acad. Sci. U.S.A. 100 (2003) 14421–14426.
[20] J. Yamauchi, Y. Miyamoto, J.R. Chan, A. Tanoue, ErbB2 directly activates the exchange factor Dock7 to promote Schwann cell migration, J. Cell Biol. 181 (2008) 351–365.
[21] K.S. Grossmann, H. Wende, F.E. Paul, C. Cheret, A.N. Garratt, S. Zurborg, K. Feinberg, D. Besser, H. Schulz, E. Peles, M. Selbach, W. Birchmeier, C. Birchmeier, The tyrosine phosphatase Shp2 (PTPN11) directs neuregulin-1/ErbB signaling throughout Schwann cell development, Proc. Natl. Acad. Sci. U.S.A. 106 (2009) 16704–16709.
[22] C. Jopling, D.I. van Geemen, J. den Hertog, Shp2 knockdown and Noonan/LEOPARD mutant Shp2-induced gastrulation defects, PLoS Genet. 3 (2007) e225.
[23] S. Hossain, G. Fragoso, W.E. Mushynski, G. Almazan, Regulation of peripheral myelination by Src-like kinases, Exp. Neurol. 226 (2010) 47–57.
[24] M. Varjosalo, S. Keskitalo, A. Van Drogen, H. Nurkkala, A. Vichalkovski, R. Aebersold, M. Gstaiger, The protein interaction landscape of the human CMGC kinase group, Cell Rep. 3 (2013) 1306–1320.

THE JOURNAL OF BIOLOGICAL CHEMISTRY VOL. 289, NO. 49, pp. 33887–33903, December 5, 2014

Arf6 Guanine Nucleotide Exchange Factor Cytohesin-2 Binds to CCDC120 and Is Transported Along Neurites to Mediate Neurite Growth*[S]

Received for publication, April 24, 2014, and in revised form, October 7, 2014 Published, JBC Papers in Press, October 17, 2014, DOI 10.1074/jbc.M114.575787

Tomohiro Torii[‡1,2], **Yuki Miyamoto**[‡], **Kenji Tago**[§], **Kazunori Sango**[¶], **Kazuaki Nakamura**[‡], **Atsushi Sanbe**[‖], **Akito Tanoue**[‡1], **and Junji Yamauchi**[‡**3]

From the [‡]Department of Pharmacology, National Research Institute for Child Health and Development, Setagaya, Tokyo 157-8535, the [§]Graduate School of Medicine, Jichi Medical University, Shimotsuke, Tochigi 329-0498, the [¶]Amyotrophic Lateral Sclerosis/Neuropathy Project, Tokyo Metropolitan Institute of Medical Science, Setagaya, Tokyo 156-8506, the [‖]School of Pharmacy, Iwate Medical University, Morioka, Iwate 020-0023, and the [**]Graduate School of Medical and Dental Sciences, Tokyo Medical and Dental University, Bunkyo, Tokyo 113-8510, Japan

Background: The Arf6 activator, cytohesin-2, is involved in neurite growth.
Results: Cytohesin-2 binds to CCDC120 and is transported along growing neurites.
Conclusion: This interaction is required for Arf6 activation and neurite growth.
Significance: The previously unknown functional CCDC120 is a new cytohesin adaptor protein, which regulates neurite growth.

The mechanism of neurite growth is complicated, involving continuous cytoskeletal rearrangement and vesicular trafficking. Cytohesin-2 is a guanine nucleotide exchange factor for Arf6, an Arf family molecular switch protein, controlling cell morphological changes such as neuritogenesis. Here, we show that cytohesin-2 binds to a protein with a previously unknown function, CCDC120, which contains three coiled-coil domains, and is transported along neurites in differentiating N1E-115 cells. Transfection of the small interfering RNA (siRNA) specific for CCDC120 into cells inhibits neurite growth and Arf6 activation. When neurites start to extend, vesicles containing CCDC120 and cytohesin-2 are transported in an anterograde manner rather than a retrograde one. As neurites continue extension, anterograde vesicle transport decreases. CCDC120 knockdown inhibits cytohesin-2 localization into vesicles containing CCDC120 and diffuses cytohesin-2 in cytoplasmic regions, illustrating that CCDC120 determines cytohesin-2 localization in growing neurites. Reintroduction of the wild type CCDC120 construct into cells transfected with CCDC120 siRNA reverses blunted neurite growth and Arf6 activity, whereas the cytohesin-2-binding CC1 region-deficient CCDC120 construct does not. Thus, cytohesin-2 is transported along neurites by vesicles containing CCDC120, and it mediates neurite growth. These results suggest a mechanism by which guanine nucleotide exchange factor for Arf6 is transported to mediate neurite growth.

In the developing nervous system, neuronal cells continuously change their morphology and undergo neurite outgrowth, axon navigation, and synaptogenesis to form neural networks (1). Neurite outgrowth is a complicated process and involves various dynamic molecular mechanisms (2–5). For example, membrane, cytoskeletal, and signaling components are continuously transported along growing neurites (6, 7).

Arfs belong to the small guanine nucleotide-binding protein family. Similar to Ras and Rho GTPases, Arfs also act as molecular switches; they are biologically active when bound to GTP and are inactive when bound to GDP. Mammalian Arfs are grouped into three classes as follows: class I (Arf1 and Arf2 and/or Arf3), class II (Arf4 and Arf5), and class III (Arf6) (8–11). Among them, Arf6 is a unique Arf protein because its primary role is to control cytoskeletal rearrangement, whereas that of the other Arfs is to regulate intracellular membrane trafficking (8, 9). Two types of proteins, guanine nucleotide exchange factors (GEFs)[4] and GTPase-activating proteins, strictly control the Arf6 guanine nucleotide-binding state. The former reaction is important because GEFs define the strength and/or the cellular compartment to activate Arf6 by integrating the upstream signals (10, 11). Cytohesin-2 is such a protein and is one of four cytohesins (12, 13). All cytohesins are composed of the same domain structure as follows: the N-terminal coiled-coil (CC) domain, the catalytic Sec7 domain, the phospho-

* This work has been supported by grants-in-aid for young scientists, Scientific Research B, and Scientific Research on Innovative Areas, "Glial Assembly: A New Regulatory Machinery of Brain Function and Disorders" from the Japanese Ministry of Education, Culture, Sports, Science, and Technology and the Japanese Ministry of Health, Labour, and Welfare, and in part by grants from the Takeda Science Foundation and the Uehara Science Foundation.
[S] This article contains supplemental Movies 1–4.
[1] Both authors contributed equally to this work.
[2] To whom correspondence may be addressed: Dept. of Pharmacology, National Research Institute for Child Health and Development, 2-10-1 Okura, Setagaya, Tokyo 157-8535, Japan. Tel.: 81-3-5494-7120 (Ext. 4670); Fax: 81-3-5494-7057; E-mail: torii-t@ncchd.go.jp.
[3] To whom correspondence may be addressed: Dept. of Pharmacology, National Research Institute for Child Health and Development, 2-10-1 Okura, Setagaya, Tokyo 157-8535, Japan. Tel.: 81-3-5494-7120 (Ext. 4670); Fax: 81-3-5494-7057; E-mail: yamauchi-j@ncchd.go.jp.

[4] The abbreviations used are: GEF, guanine nucleotide exchange factor; CC, coiled-coil; RFP, red fluorescent protein; PH, pleckstrin homology; ANOVA, analysis of variance; EGFP, enhanced GFP.

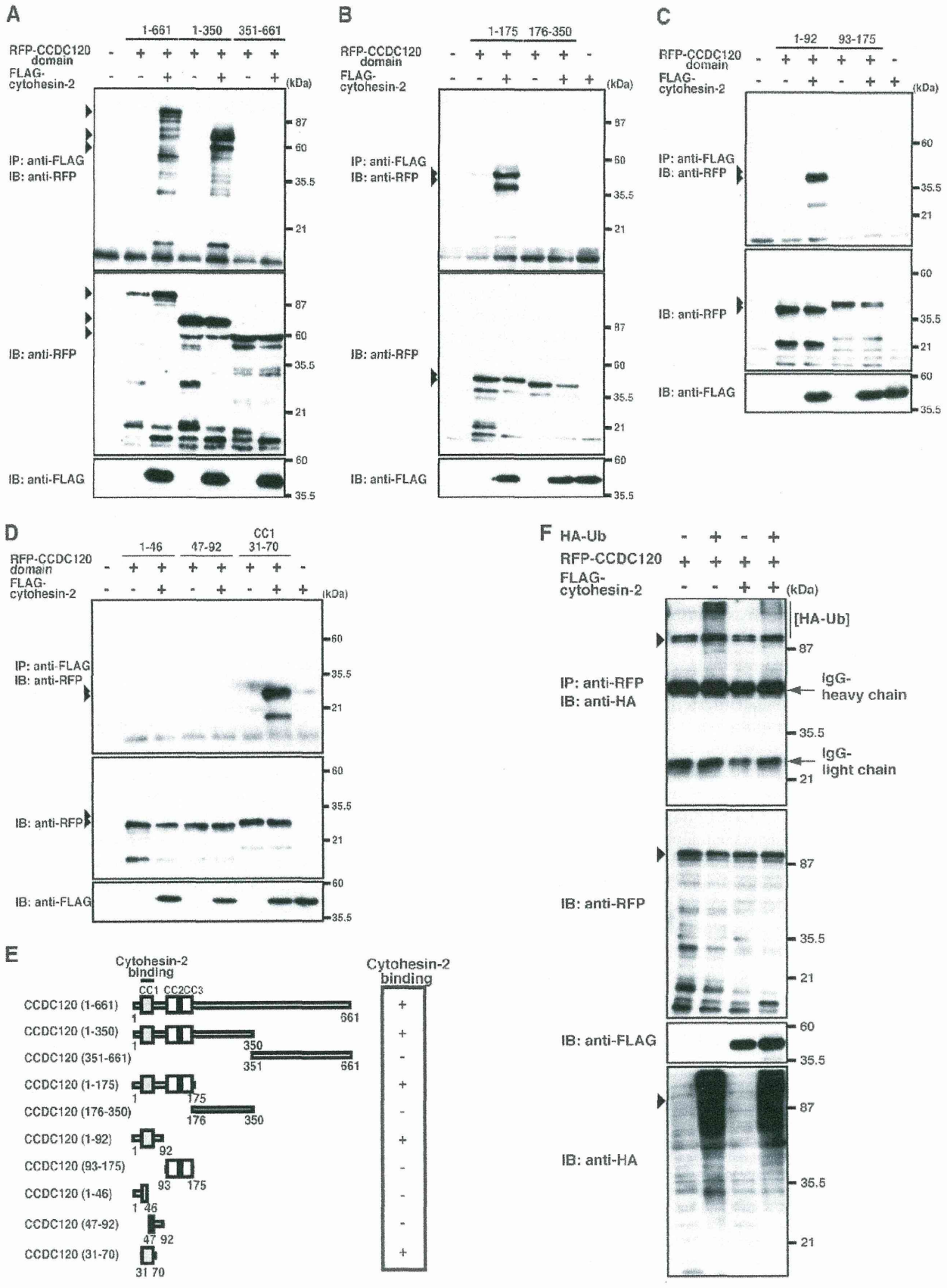

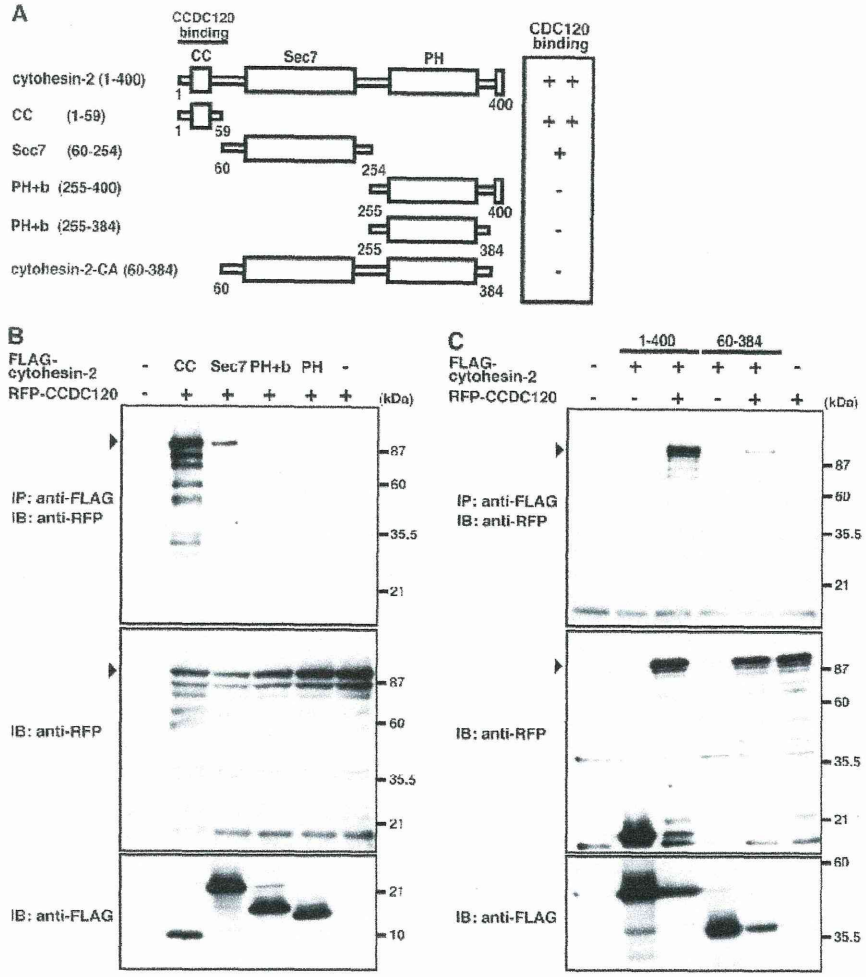

FIGURE 2. **Interaction of cytohesin-2 and CCDC120 are mediated by the CC domain of cytohesin-2 in mammalian cells.** *A*, schematic structures of full-length (wild type) cytohesin-2 and the domains are illustrated (number shows amino acid's one). *B* and *C*, 293T cells were transfected with plasmids coding either FLAG-tagged CCDC120 domain (full-length(1–400), CC(1–59), Sec7(60–254), PH+b(255–400), PH(255–384), and cytohesin-2-CA(60–384 amino acids)) or RFP-CCDC120. Cytohesin-2-CA is characterized as a constitutively active form of cytohesin-2 in previous study (14). After 48 h, cells were lysed. Cell lysates were immunoprecipitated (*IP*) with an anti-FLAG antibody and immunoblotted (*IB*) with an anti-RFP antibody. The total lysates were also used for immunoblotting with an anti-RFP antibody or anti-FLAG antibody. *Arrowheads* indicate the position of RFP fusion proteins.

inositide-binding pleckstrin homology (PH) domain, and the C-terminal polybasic amino acid region (14).

We previously reported that cytohesin-2 and downstream Arf6 activation participate in promoting neurite extension (15) and that cytohesin-2 regulates its extension through the cytoskeletal protein actinin at the growth cone in mouse neuroblastoma N1E-115 cells (16). However, the mechanism of Arf6-GEF cytohesin-2 transport along growing neurites has not been resolved. In this study, we demonstrate that a protein, CC domain-containing protein 120 (CCDC120), which had a previously unknown function, is the binding partner that determines cytohesin-2 localization and mediates Arf6 activation and neurite growth. Cytohesin-2 is transported along growing neurites in vesicles containing CCDC120. These results present

FIGURE 1. **CCDC120 binds to cytohesin-2 through the CC1 domain.** *A*, 293T cells were transfected with plasmids coding either RFP-tagged CCDC120 region (1–661, 1–350, and 351–661 amino acids) or FLAG-cytohesin-2. After 48 h, cells were lysed. Cell lysates were immunoprecipitated (*IP*) with an anti-FLAG antibody and immunoblotted with an anti-RFP antibody. The total lysates were also used for immunoblotting (*IB*) with an anti-RFP antibody or anti-FLAG antibody. *Arrowheads* indicate the position of RFP fusion proteins. *B*, 293T cells were transfected with plasmids coding either RFP-tagged CCDC120 region (1–175 and 176–350 amino acids) or FLAG-cytohesin-2. After 48 h, cells were lysed. Cell lysates were immunoprecipitated with an anti-FLAG antibody and immunoblotted with an anti-RFP antibody. The total lysates were also used for immunoblotting with an anti-RFP antibody or anti-FLAG antibody. *Arrowheads* indicate the position of RFP fusion proteins. *C*, 293T cells were transfected with plasmids coding either RFP-tagged CCDC120 region (1–92 and 93–175 amino acids) or FLAG-cytohesin-2. After 48 h, cells were lysed. Cell lysates were immunoprecipitated with an anti-FLAG antibody and immunoblotted with an anti-RFP antibody. The total lysates were also used for immunoblotting with an anti-RFP antibody or anti-FLAG antibody. *Arrowheads* indicate the position of RFP fusion proteins. *D*, 293T cells were transfected with the plasmids coding for FLAG-tagged cytohesin-2 with or without either of the RFP-tagged CCDC120 domains. After 48 h, cells were lysed. The immunoprecipitates with an anti-FLAG antibody were immunoblotted with an anti-RFP antibody. Total expressed proteins are also shown. *Arrowheads* indicate the position of RFP-CCDC120 domains. *E*, schematic structures of wild type full-length CCDC120 and their domains (*numbers* indicate domains of the amino acid). *F*, 293T cells were transfected with plasmids coding either RFP-tagged full-length CCDC120, FLAG-tagged cytohesin-2, or HA-tagged ubiquitin. After 48 h, cells were lysed. Cell lysates were immunoprecipitated with an anti-RFP antibody and immunoblotted with an anti-HA antibody. The total lysates were also used for immunoblotting with an anti-RFP antibody, anti-HA antibody, or anti-FLAG antibody. *Arrowheads* indicate the position of RFP-fusion full-length CCDC120.

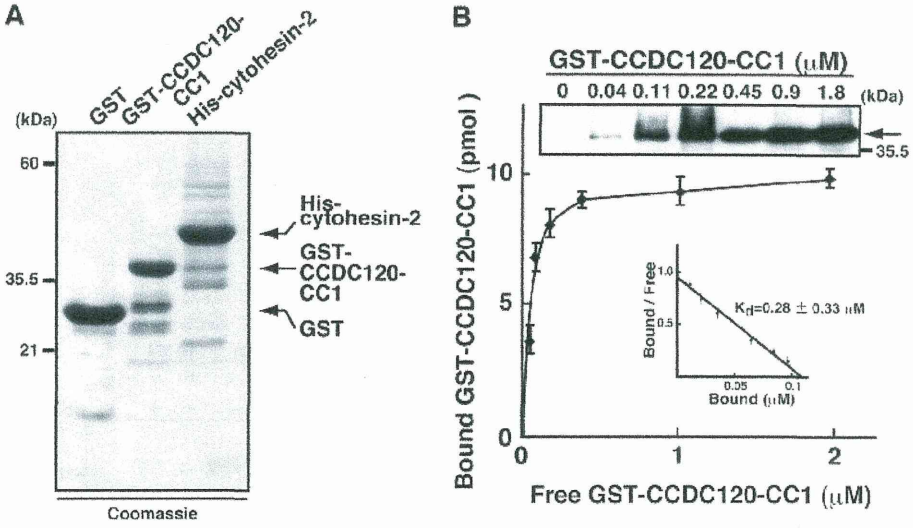

FIGURE 3. **Direct binding of GST-CCDC120-CC1 to cytohesin-2.** *A*, recombinant GST, GST-CCDC120-CC1, and His-cytohesin-2 were purified from *E. coli* and stained with Coomassie Brilliant Blue. *Arrows* indicate GST, GST-CCDC120-CC1, or His-cytohesin-2. *B*, quantitative analysis of the interaction between GST-CCDC120-CC1 and His-cytohesin-2 was performed. Various concentrations (0.04 to 1.8 μM) of recombinant GST-CCDC120-CC1 were added to an immobilized His-cytohesin-2 (0.5 μg) in 500 μl of buffer. Bound GST-CCDC120-CC1 (indicated by an *arrow*) was detected by immunoblotting with an anti-GST antibody. Amounts of the free and bound GST fusion protein were calculated by determining the protein amounts from the supernatant and pellet fractions. The amount of bound *versus* free GST-CCDC120-CC1 was plotted in a line graph (see *inset*). Scatchard analysis indicates that the K_d value was 0.28 ± 0.033 μM. Results are means ± S.D. for three independent experiments.

evidence of how a GEF for Arf6 is transported to mediate Arf6 activation and neurite growth.

EXPERIMENTAL PROCEDURES

Antibodies—Rabbit polyclonal CCDC120 antibody was purchased from ProteinTech (Chicago, IL; 1:500 for immunoblotting and immunofluorescence). Rabbit serum for cytohesin-2 was generated against a CRKKRISVKKKQEQ peptide, which was synthesized by IWAKI (Tokyo, Japan). The polyclonal anti-cytohesin-2 antibody was affinity-purified using an antigen peptide-conjugated resin and used for immunoblotting (1:500). The mouse monoclonal cytohesin-2 was purchased from Santa Cruz Biotechnology (1:50 for immunofluorescence). The mouse monoclonal active Arf6 was purchased from NewEast BioScience (Malvern, PA; 1:100 for immunofluorescence). The following antibodies (dilution used for immunoblotting) were purchased: mouse monoclonal anti-Arf6 (1:50; Santa Cruz Biotechnology); mouse monoclonal and rabbit polyclonal anti-GFP (1:1,000; MBL, Nagoya, Japan); rabbit polyclonal anti-RFP (1:1,000; Evrogen, Moscow, Russia); mouse monoclonal anti-FLAG (1:1,000; Sigma); mouse monoclonal anti-β-actin (1:1,000; BD Biosciences); horseradish peroxidase-labeled secondary antibodies (1:10,000; GE Healthcare); and fluorescence-labeled secondary antibodies (1:500; Invitrogen).

Plasmids for Mammalian Cell Expression—The pRK5-HA-ubiquitin plasmid was purchased from Addgene (Cambridge, MA). The p3×FLAG-cytohesin-2 and the plasmids encoding the domain were constructed as described in our previous reports (16–18). Human CCDC120 cDNA was obtained from the Biological Resource Center of the National Institute of Technology and Evaluation (Chiba, Japan). The domains (amino acids 1–350, 351–661, 1–175, 176–350, 1–92, 93–175, 1–46, 47–92, and amino acids 31–70) were constructed using PCR and inserted into pTagRFP-C vector (Evrogen). The CCDC120-ΔCC1 mutant (deleted amino acids 31–70) was also produced using PCR and subcloned into pTagRFP-C. Rab8b, Rab11, VAMP2, VAMP4, and VAMP7 were amplified in N1E-115 cell cDNA by the PCR method and subcloned into pEGFP-C1 vectors. All nucleotide sequences were confirmed by the Fasmac sequencing service (Kanagawa, Japan).

Recombinant Proteins—Recombinant GST and GST-GGA3 (16, 17) were produced using *Escherichia coli* BL21(DE3)pLysS (TaKaRa Bio, Kyoto, Japan) and purified according to the manufacturer's protocol for a glutathione-Sepharose 4B (GE Healthcare). Recombinant GST-CCDC120-CC1 (amino acids 31–70) was also purified using *E. coli* BL21(DE3)pLysS. The pET42a vector-based transformed *E. coli* was treated with 0.4 mM isopropyl 1-thio-β-D-galactopyranoside at 30 °C for 2.5 h and harvested by centrifugation. The precipitates were extracted with buffer A (50 mM Tris-HCl (pH 7.5), 5 mM $MgCl_2$, 1 mM dithiothreitol, 1 mM phenylmethanesulfonyl fluoride, 1 mg/ml leupeptin, 1 mM EDTA, and 0.5% Nonidet P-40) containing 500 μg/ml lysozyme and 100 μg/ml DNase I on ice. All purification steps were performed at 4 °C. The centrifuged supernatants were applied to a glutathione-Sepharose 4B column (GE Healthcare). The resins were washed with buffer B (100 mM Tris-HCl (pH 8.0), 2 mM $MgCl_2$, 1 mM dithiothreitol, 1 mM phenylmethanesulfonyl fluoride, and 1 μg/ml leupeptin). Recombinant proteins were eluted with buffer B containing 20 mM glutathione. The eluted fractions were dialyzed against buffer C (10 mM HEPES-NaOH (pH 7.5), 1 mM dithiothreitol, 2 mM $MgCl_2$, 1 mM dithiothreitol, 1 mM phenylmethanesulfonyl fluoride, 1 μg/ml leupeptin, and 150 mM NaCl) and stored at −80 °C until use. Recombinant His-tagged cytohesin-2 was produced using *E. coli* BL21(DE3)pLysS and purified according to the manufacturer's protocol for a nickel-nitrilotriacetic acid resin (GE Healthcare). In brief, *E. coli* was lysed in

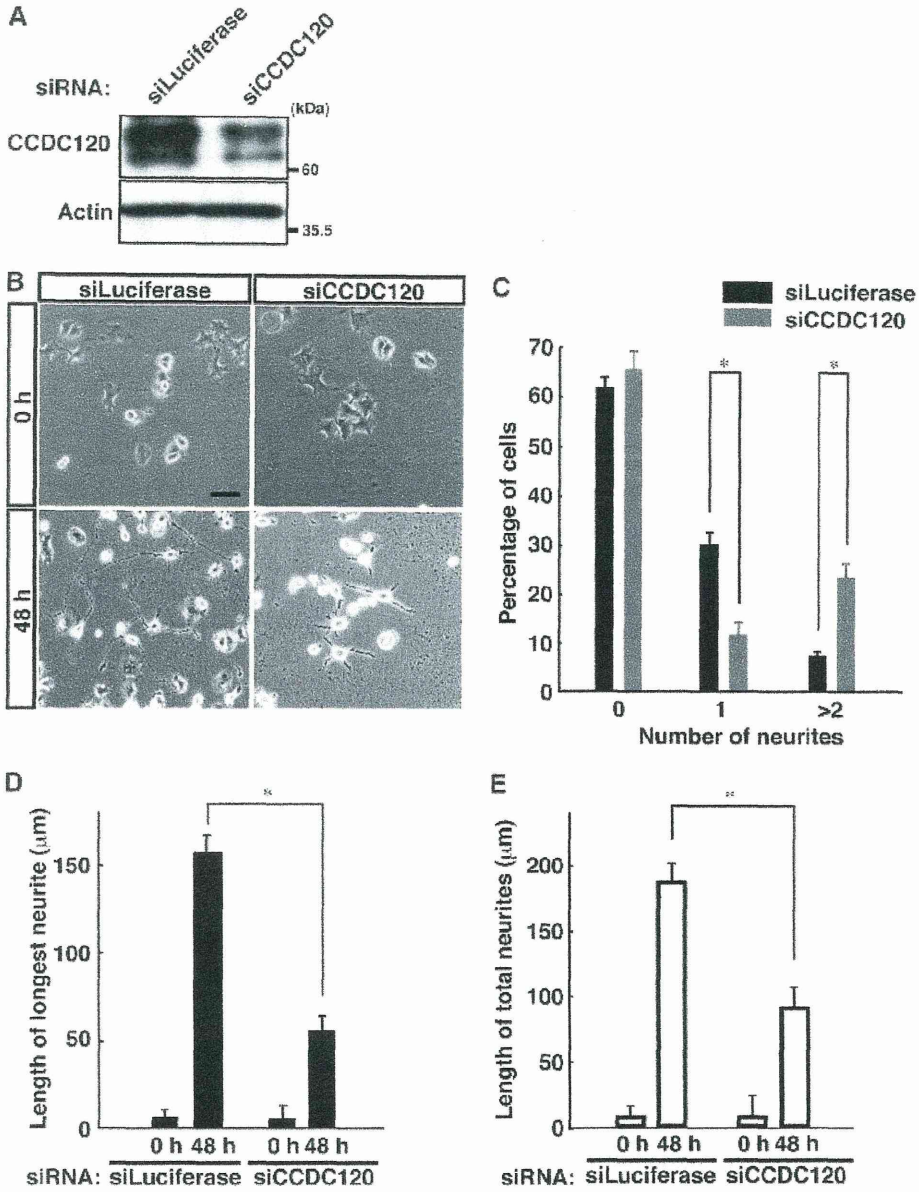

FIGURE 4. **CCDC120 is involved in neurite growth in N1E-115 cells.** *A*, N1E-115 cells were transfected with an siRNA for control luciferase or CCDC120. The expression levels of CCDC120 and actin were examined with immunoblotting using the respective antibodies. *B* and *C*, N1E-115 cells were transfected with an siRNA for control luciferase or CCDC120. Representative images are also shown at 48 h following induction of differentiation. Cells with processes longer than two cell bodies were counted as cells bearing neurites. Knockdown of CCDC120 decreased the numbers of cells with a single neurite and increased the numbers of cells with multiple neurites. *Scale bars*, 10 μm. Data were evaluated using a one-way ANOVA (*, $p < 0.01$; $n = 3$ microscopic fields). *D* and *E*, CCDC120 knockdown also decreased the length of longest neurites and the total length of neurites. Data were evaluated using a one-way ANOVA (*, $p < 0.01$; $n = 50$ cells).

lysis buffer A and centrifuged. The supernatant was mixed with nickel-nitrilotriacetic acid resin. Bound His-tagged cytohesin-2 proteins were extensively washed with lysis buffer A containing 500 mM NaCl followed by lysis buffer containing 500 mM NaCl and 50 mM EDTA, and subsequently eluted with lysis buffer containing 10 mM imidazole (Nacalai Tesque), according to the manufacturer's protocol. The aliquot was stored at −80 °C until use.

siRNA Oligonucleotides—The 21-nucleotide siRNA duplexes were synthesized using Nippon EGT (Toyama, Japan). The specific target sequences were as follows: 5′-AAGATGGCAATGGGCAGGAAG-3′ for mouse cytohesin-2 siRNA and 5′-AAGCAGCAGAGGAAGACGTTC-3′ for mouse CCDC120 siRNA. The target sequence of the control *Photinus pyralis* luciferase siRNA was 5′-AAGCCATTCTATCCTCTAGAG-3′, which does not have significant homology to any mammalian gene sequences.

Cell Cultures—Mouse N1E-115 neuroblastoma cells and human embryonic kidney 293T cells were cultured on cell culture dishes at 37 °C in DMEM containing 10% heat-inactivated FBS, 50 units/ml penicillin, and 50 μg/ml streptomycin. For induction of differentiation, cells were cultured in normal medium in the absence of serum. Cells with processes longer than two cell bodies were counted as cells bearing neurites at 48 h after deprivation of serum.